

Synthesis and Characterization of Binuclear Cu(II) Complex with 22-Membered Phenol-Based N₄O₂ Compartmental Macrocyclic Ligand

Chung-Hun Han, Ki-Ju Kim, and Jong-Chul Byun

Department of Chemistry, College of Natural Science, Cheju National University

Abstract. A dinuclear copper(II) complex, Cu₂([22]-HMTADO)(H₂O)₄]Cl₂ · 8H₂O, with [2+2] symmetrical N₄O₂ compartmental macrocyclic ligand {H₂[22]-HMTADO: 5,5,11,17,17,23-hexamethyl-3,7,15,19-tetraazatricyclo[19.3.1.1^{9,13}]hexacos-1(25),2,7,9,11,13(26),14,19,21,23-decane-25,26-diol} containing bridging phenolic oxygen atoms was synthesized by condensation of 2,6-diformyl-*p*-cresol and 2-dimethyl-1,3-propandiamine, in CuCl₂. Single-crystal X-ray diffraction studies are reported for [Cu₂([22]-HMTADO)(H₂O)₄]Cl₂ · 10H₂O. The complex crystallized in the monoclinic system, space group *C2/m*, *a* = 16.3781(6) Å, *b* = 25.3716(9) Å, *c* = 9.9589(3) Å, *β* = 96.3570(10)°, and *Z* = 4. Octahedral two copper ions stereochemistries are observed with axially coordinated water molecules. The structure of the complexes has been elucidated by elemental analysis, molar conductance, mass, IR, electronic studies.

Key words : copper complex, compartmental macrocyclic ligand

1. Introduction

Interest in exploring metal ion complexes with macrocyclic ligands has been continually increasing owing to the recognition of their role played by these structures in metalloproteins. Schiff base macrocycles have been of great importance in macrocyclic chemistry. They were among the first artificial metal macrocyclic complexes to be synthesized. The metal complexes containing synthetic macrocyclic ligands have attracted a great deal of attention because they can be used as models for more intricate biological macrocyclic systems: metalloporphyrins (hemoglobin, myoglobin, cytochrome, chlorophyll),

corrins (vitamin B₁₂) and antibiotics (valinomycin, nonactin). These discoveries have created supramolecular chemistry and its enormous diversity [1-5].

Over the past decade, many studies have been focused on the design, template synthesis and characterization of the new supramolecular polyaza and polyoxaaza Schiff base mono- and homo- or heterodinuclear macrocyclic complexes of metal ions of varying radii and electron configuration - in particular rare earth elements - and the factors which prove to be of importance in directing the synthetic pathway in these systems.

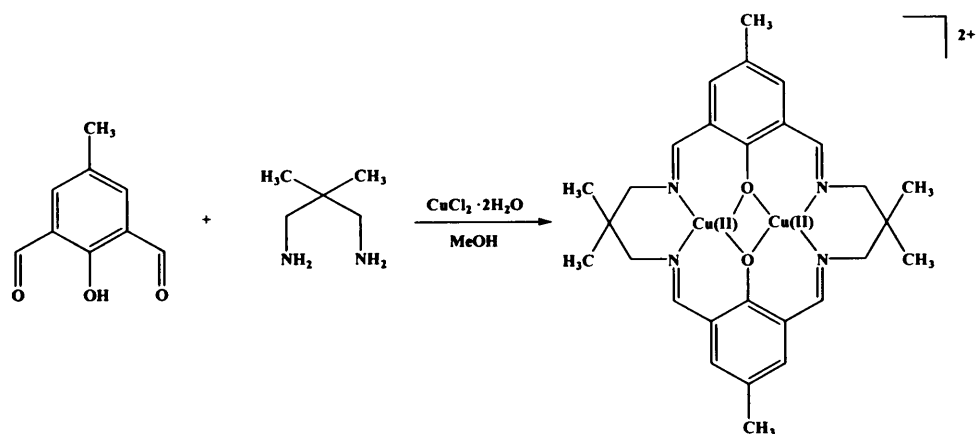
Macrocyclic Schiff bases have been widely studied because they can selectively chelate certain metal ions depending on the number, type and position of their donor atoms, the ionic radius of the metal center, and coordinating properties of counter ions.

Recognition of the importance of complexes containing macrocyclic ligands for supramolecular science, bioinorganic chemistry, biomedical applications, separation and encapsulation processes as well as formation of compounds with unusual properties and structures has led to considerable effort to develop methods for the synthesis of these compounds. The macrocyclic complex is formed by adding the required metal ion to a preformed macrocycle. However, the direct synthesis of macrocycles often results in very low yield of the desired product with the domination of competing linear polymerization or other side reactions.

Many synthetic routes to macrocyclic ligands involve the use of the metal ion template to orient the reacting groups of linear substrates in the desired conformation for the ring to close. The favorable enthalpy for the formation of metal-ligand bonds overcomes the unfavorable entropy of the ordering of the multidentate ligand around the metal ion and hence it promotes the cyclization reaction [1, 6, 7]. The effective method for the synthesis of Schiff base macrocyclic complexes which involves the condensation reaction between suitable dicarbonyl compounds and primary diamines carried out in the presence of appropriate metal ions which serve as templates in directing the steric course of the reaction. In this metal template effect the metal ion - through coordination -

organizes the linear substrates to facilitate the condensation process which may lead toward either [1 + 1] or [2 + 2] macrocyclic products.

Whether the cyclization proceeds through an intramolecular condensation to give a [1 + 1] macrocycle or through the bimolecular steps leading to a [2 + 2] macrocycle depends on the relative proportions of linear substrates, the nature of the cation and reactants (chain length, number and location of potential donor atoms), the ratio of the template ionic radius to the cavity size, conformation of acyclic intermediates and coordination properties of counter ions. Rare earth metal ions have found to be very efficient metal templates in the synthesis of the complexes of this type. The first example of such an action of these ions in the synthesis of polyaza Schiff base macrocyclic compounds was reported for scandium(III) ion [8]. Rare earth elements are known to have little or no stereochemical requirements and can be accommodated by the stereochemical constraints enforced by the template process. In some cases the mononuclear or dinuclear open-chain chelates with two terminal carbonyl groups or one terminal carbonyl group and one terminal amine group - considered as potential intermediates in the template process [1, 6, 7] - can be the final products of the Schiff base condensation. The formation of these compounds instead of the expected macrocycles may be attributed to the unfavorable positioning of the terminal groups which decreases the probability of intermolecular linkage with next diamine molecule or a possibility of the nucleophilic attack of the amine nitrogen on the carbon atom of the



Scheme 1. Synthesis of the binuclear Cu(II) complex of phenol-based macrocyclic ligand ($H_2[22]$ -HMTADO).

carbonyl group and stabilizes the open-chain product once formed. The investigation of the mechanism of the formation of Schiff base complexes demonstrates that the structure and coordination mode of potential intermediates is one of the key factors that determine the preferred pathway of the metal-ion templated condensation in the Schiff base systems and must be taken into account in the design and synthesis of desired products.

This work performs synthesis and physico-chemical characterization of dinuclear copper(II) complex with [2+2] symmetrical N_4O_2 compartmental macrocyclic ligand ($H_2[22]$ -HMTADO : 5,5,11,17,17,23-hexamethyl-3,7,15,19-tetraazatricyclo [19,3,1,1^{9,13}]hexacosa-1(25),2,7,9,11,13(26),14,19,21,23-decane-25,26-diol} containing bridging phenolic oxygen atoms was synthesized by condensation of 2,6-diformyl-*p*-cresol, 2-dimethyl-1,3-propanediamine, and $CuCl_2$ (Scheme 1). Single-crystal X-ray diffraction studies are reported for $[Cu_2([22]-HMTADO)(H_2O)_4]Cl_2 \cdot 10H_2O$.

II. Experimental

1. Chemicals and Physical Measurements

All chemicals were commercial analytical reagents and were used without further purification. For the spectroscopic and physical measurements, organic solvents were dried and purified according to the literature methods. Nanopure quality water was used throughout this work. Microanalyses of C, H, and N was carried out using LECO CHN-900 analyzer. Conductance measurement of the complex was performed at $25 \pm 1^\circ C$ using an ORION 162 conductivity temperature meter. IR spectrum was recorded with a Bruker FSS66 FT-IR spectrometer in the range $4000 - 370 \text{ cm}^{-1}$ using KBr pellets. Electronic absorption spectrum was measured at $25^\circ C$ on a UV-3150 UV-VIS-NIR Spectrophotometer (SHIMADZU). FAB-mass spectrum was obtained on a JEOL JMS-700 Mass Spectrometer using argon (6kV, 10mA) as the FAB gas. The accelerating

voltage was 10kV and glycerol was used as the matrix. The mass spectrometer was operated in positive ion mode and mass spectrum was calibrated by Alkali-CsI positive.

2. Preparations

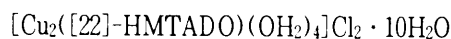
1) 2,6-diformyl-*p*-cresol.

The synthesis of 2,6-diformyl-*p*-cresol was prepared according to the literature methods previously reported [9, 10].

2) $[\text{Cu}_2(\text{[22]-HMTADO})(\text{H}_2\text{O})_4]\text{Cl}_2 \cdot 8\text{H}_2\text{O}$.

A methanolic solution (30 mL) of 2,6-diformyl-*p*-cresol (1.312 g) was added to a suspension of the 2,2-dimethyl-1,3-propanediamine (0.824 g) and the cupric chloride dihydrate (1.364 g) in methanol (30 mL). The mixture was refluxed for 20 min whereupon the solution turned immediately to dark green, and then the solvent was partially evaporated. The pale green precipitate obtained by addition of tetrahydrofuran (200 mL) filtered, washed with tetrahydrofuran and dried in vacuo. The products can be further purified by hot water. Yield: 92%. Anal. Calcd (Found) % for $\text{C}_{28}\text{H}_{38}\text{N}_4\text{O}_{14}\text{Cl}_2\text{Cu}_2$: C, 38.53 (38.51); H, 6.70 (6.38); N, 6.42 (6.46). M (water): 218 $\text{ohm}^{-1}\text{cm}^2\text{mol}^{-1}$.

3. Crystallography of the



Suitable crystals of $[\text{Cu}_2(\text{[22]-HMTADO})(\text{OH}_2)_4]\text{Cl}_2 \cdot 10\text{H}_2\text{O}$ were obtained by slow evaporation of hot aqueous solution of $[\text{Cu}_2(\text{[22]-HMTADO})(\text{OH}_2)_4]\text{Cl}_2 \cdot 8\text{H}_2\text{O}$ complex at

atmospheric pressure. The dark green crystal of $[\text{Cu}_2(\text{[22]-HMTADO})(\text{OH}_2)_4]\text{Cl}_2 \cdot 10\text{H}_2\text{O}$ was attached to glass fibers and mounted on a Bruker SMART diffractometer equipped with a graphite monochromated Mo $K\alpha$ ($\lambda = 0.71073 \text{ \AA}$) radiation, operating at 50 kV and 30 mA and a CCD detector : 45 frames of two-dimensional diffraction images were collected and processed to obtain the cell parameters and orientation matrix. The crystallographic data, conditions for the collection of intensity data, and some features of the structure refinements are listed in Table 1. The intensity data were corrected for Lorentz and polarization effects. Absorption correction was not made during processing. Of the 13200 unique reflections measured, 4935 reflections in the range $2.06^\circ \leq \theta \leq 28.29^\circ$ were considered to be observed ($I > 2\sigma(I)$) and were used in subsequent structure analysis. The program SAINTPLUS [11] was used for integration of the diffraction profiles. The structures were solved by direct methods using the SHELXS program of the SHELXTL package [12] and refined by full matrix least squares against F^2 for all data using SHELXL. All non-H atoms were refined with anisotropic displacement parameters. Hydrogen atoms were placed in idealized positions [$U_{\text{iso}} = 1.2U_{\text{eq}}$ (parent atom)].

III. Results and discussion

1. Description of the structure

An ORTEP view of $[\text{Cu}_2(\text{[22]-HMTADO})(\text{OH}_2)_4]\text{Cl}_2 \cdot 10\text{H}_2\text{O}$ is shown in Fig. 1, and

bond distances and angles are summarized in Table 2 and 3. The crystal structure of this complex is composed of binuclear cation of the indicated formula and noninteracting chloride anions. These results are backed up by the molar conductivity ($\Lambda_M = 218 \text{ ohm}^{-1} \text{ cm}^2 \text{ mol}^{-1}$) which agreed with assignment of the structure as $[\text{Cu}_2(\text{[22]-HMTADO})(\text{OH}_2)_4]\text{Cl}_2 \cdot 10\text{H}_2\text{O}$. The binuclear cation, $[\text{Cu}_2(\text{[22]-HMTADO})(\text{OH}_2)_4]^{2+}$ shows two octahedral environment,

where the copper(II) ions are coordinated by the two oxygen atoms of water molecules of the copper basal planes (CuN_2O_2) in trans positions, respectively.

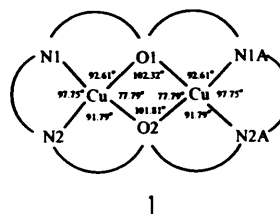


Table 1. Crystal data and structure refinement for $[\text{Cu}_2(\text{[22]-HMTADO})(\text{H}_2\text{O})_4]\text{Cl}_2 \cdot 10\text{H}_2\text{O}$

Empirical formula	$\text{C}_{28}\text{H}_{62}\text{Cl}_2\text{Cu}_2\text{N}_4\text{O}_{16}$	
Formula weight	908.80	
Temperature	173(2) K	
Wavelength	0.71073 Å	
Crystal system	Monoclinic	
Space group	$C2/m$	
Unit cell dimensions	$a = 16.3781(6)$ Å	$\alpha = 90^\circ$
	$b = 25.3716(9)$ Å	$\beta = 96.3570(10)^\circ$
	$c = 9.9589(3)$ Å	$\gamma = 90^\circ$
Volume	$4112.9(2)$ Å ³	
Z	4	
Density (calculated)	1.468 g/cm ³	
Absorption coefficient	1.233 mm ⁻¹	
$F(000)$	1912	
Crystal size	0.50 x 0.30 x 0.20 mm ³	
Theta range for data collection	2.06 to 28.29°	
Index ranges	$-21 \leq h \leq 17$, $-33 \leq k \leq 26$, $-13 \leq l \leq 13$	
Reflections collected	13200	
Independent reflections	4935 [$R(\text{int}) = 0.0393$]	
Completeness to $\theta = 28.29^\circ$	94.3 %	
Absorption correction	None	
Refinement method	Full-matrix least-squares on F^2	
Data / restraints / parameters	4935 / 0 / 249	
Goodness-of-fit on F^2	1.094	
Final R indices [$I > 2\sigma(I)$]	$R_1 = 0.0336$, $wR_2 = 0.0803$	
R indices (all data)	$R_1 = 0.0394$, $wR_2 = 0.0834$	

$$R = \frac{\sum |F_o| - |F_c|}{\sum |F_o|}, R_w = \frac{[\sum w(F_o^2 - F_c^2)^2 / \sum w(F_o^2)^2]}{2}$$

$$w = 1/[\sigma^2(F_o^2) + (0.0282P)^2 + 7.1613P] \text{ where } P = (F_o^2 + 2F_c^2)/3.$$

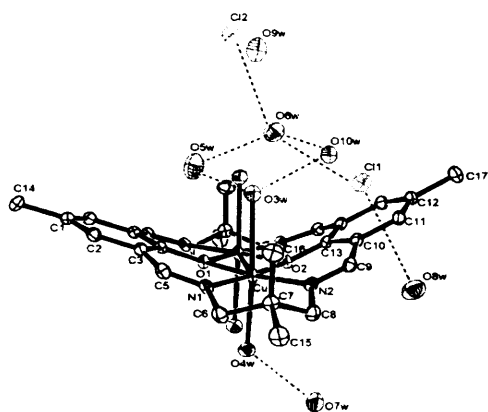


Fig. 1. Structural representation of core structure (top view) for the $[\text{Cu}_2([\text{22}]\text{-HMTADO})(\text{OH}_2)_4]\text{Cl}_2 \cdot 10\text{H}_2\text{O}$ complex.

The macrocyclic complex adopts an essentially flat structure with the two octahedral copper centers bridged by the two phenoxide oxygen atoms, with quite large Cu-O-Cu angles ($102.32(8)^\circ$ and $101.81(7)^\circ$) (1).

Magnetostructural correlations in binuclear copper(II) complexes bridged equatorially by pairs of hydroxide groups show that the major factor controlling spin coupling between the $S=1/2$ metal centers is the Cu-O-Cu angle. The sum of angles at the phenoxide oxygens is almost exactly 360° (359.71°), indicating no square oxygen distortion. The sum of angles at the copper basal planes (CuN_2O_2) is almost exactly 360° (359.97°), indicating no plane distortion.

The copper centers are separated by $3.0482(4)$ Å. The Cu-N (imines) bond distances are in the range of $1.9490(15)$ and $1.9503(15)$ Å, and Cu-O (phenolic) are $1.9567(11)$ Å and $1.9638(11)$ Å. The Cu-O (aqua) bond distances are in the range of $2.4792(14)$ and $2.5798(14)$ Å. The bond angles N(2)-Cu-O(1), N(1)-Cu-O(2), and O(4W)-Cu-O(3W) are $169.15(6)^\circ$, $170.36(6)^\circ$ and $172.68(5)^\circ$, respectively. In this complex Cu-N (imines) and Cu-O (phenolic) distances

are shorter than Cu-O (aqua) and the angle N(2)-Cu-O(1), N(1)-Cu-O(2), and O(4W)-Cu-O(3W) are smaller than the ideal value of 180° .

Table 2. Bond lengths (Å) for $[\text{Cu}_2([\text{22}]\text{-HMTADO})(\text{OH}_2)_4]\text{Cl}_2 \cdot 10\text{H}_2\text{O}$

Cu(1)-N(1)	1.9490(15)
Cu(1)-N(2)	1.9503(15)
Cu(1)-O(1)	1.9567(11)
Cu(1)-O(2)	1.9638(11)
Cu(1)-O(4W)	2.4792(14)
Cu(1)-O(3W)	2.5798(14)
Cu(1)-Cu(1)#1	3.0482(4)
O(1)-Cu(1)#1	1.9567(11)
O(2)-Cu(1)#1	1.9638(11)

Symmetry transformations used to generate equivalent atoms: #1 : x, -y+1, z.

Table 3. Angles [$^\circ$] for $[\text{Cu}_2([\text{22}]\text{-HMTADO})(\text{OH}_2)_4]\text{Cl}_2 \cdot 10\text{H}_2\text{O}$

N(1)-Cu(1)-N(2)	97.75(7)
N(1)-Cu(1)-O(1)	92.61(6)
N(2)-Cu(1)-O(1)	169.15(6)
N(1)-Cu(1)-O(2)	170.36(6)
N(2)-Cu(1)-O(2)	91.79(6)
O(1)-Cu(1)-O(2)	77.79(6)
N(1)-Cu(1)-O(4W)	90.40(6)
N(2)-Cu(1)-O(4W)	94.49(6)
O(1)-Cu(1)-O(4W)	88.63(6)
O(2)-Cu(1)-O(4W)	90.25(6)
N(1)-Cu(1)-O(3W)	92.03(6)
N(2)-Cu(1)-O(3W)	92.03(6)
O(1)-Cu(1)-O(3W)	84.36(6)
O(2)-Cu(1)-O(3W)	86.22(6)
O(4W)-Cu(1)-O(3W)	172.68(5)
N(1)-Cu(1)-Cu(1)#1	131.37(4)
N(2)-Cu(1)-Cu(1)#1	130.87(4)
O(1)-Cu(1)-Cu(1)#1	38.84(4)
O(2)-Cu(1)-Cu(1)#1	39.10(4)
O(4W)-Cu(1)-Cu(1)#1	86.66(3)
O(3W)-Cu(1)-Cu(1)#1	86.55(3)
Cu(1)-O(1)-Cu(1)#1	102.32(8)
Cu(1)#1-O(2)-Cu(1)	101.81(7)

Symmetry transformations used to generate equivalent atoms: #1 : x, -y+1, z.

indicating that the donor atoms are not able to achieve the axial positions of a perfect octahedron : this is elongated owing to the Jahn-Teller effect and steric effect.

An angle of 29.61° exists between the benzene mean planes of macrocycle and the copper basal planes. This is bent owing to the chair conformation effect of the six-membered ring with trimethylene chain linking the azomethine nitrogen donors and copper. The two methyl groups (C(15) and C(15A)) attached to the trimethylenes are situated eclipsed conformation.

In general, hydrogen bonding plays a principal role in the packing of the title compound. There are four types of H-bonds : between coordinated waters, coordinated water - lattice water, chloride ion - lattice water, and between lattice waters (Table 4). These interactions result in a formation of polymeric

chains (Fig. 2). This chain forms a related layer structure, but within the layers binuclear cation $[\text{Cu}_2(\text{[22]-HMTADO})(\text{OH}_2)_4]^{2+}$ ions arrange zig-zag configurations.

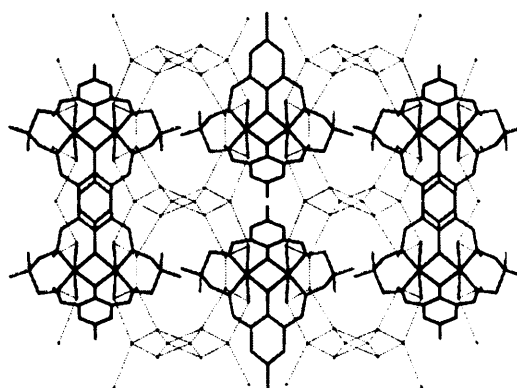


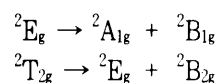
Fig. 2. The molecular packing diagram of $[\text{Cu}_2(\text{[22]-HMTADO})(\text{OH}_2)_4]\text{Cl}_2 \cdot 10\text{H}_2\text{O}$. The hydrogen bonds are indicated by dotted lines.

Table 4. Selected bond lengths (Å) and angles($^\circ$) for hydrogen bond of $[\text{Cu}_2(\text{[22]-HMTADO})(\text{OH}_2)_4]\text{Cl}_2 \cdot 10\text{H}_2\text{O}$

D-H...A	d(D-H)	d(H...A)	<DHA	d(D...A)
between coordinated waters				
O3W-H3C...O3W [x, -y+1, z]	0.897	1.876	160.45	2.738
O4W-H2C...O4W [x, -y+1, z]	0.91	1.852	174.75	2.759
coordinated water - lattice water				
O3W-H3A...O5W	0.789	2.001	165.9	2.773
O3W-H3B...O10W	0.737	2.141	157.69	2.836
O4W-H4A...O7W	0.717	2.023	162.33	2.715
O4W-H4B...O9W [-x+1/2, -y+1/2, -z+1]	0.788	2.141	161.92	2.9
O5W-H5C...O3W	0.819	1.982	162.09	2.773
chloride ion - lattice water				
O6W-H6C...Cl2	0.784	2.476	179.69	3.261
O6W-H6D...Cl1	0.845	2.423	167.38	3.252
O8W-H8C...Cl1	0.825	2.391	170.17	3.207
O8W-H8D...Cl2 [x, y, z+1]	0.91	2.311	165.92	3.202
between lattice waters				
O5W-H5B...O6W	0.869	2.094	155.5	2.907
O7W-H7A...O8W [-x+1/2, -y+1/2, -z+2]	0.965	1.909	159.73	2.834
O7W-H7B...O5W [x, y, z+1]	0.735	1.983	162.69	2.693
O9W-H9B...O8W [x, y, z-1]	0.808	2.03	172.6	2.833
O10W-H10A...O6W	0.783	2.101	166.62	2.869

2. Electronic absorption spectrum

The electronic absorption spectra of $[\text{Cu}_2([\text{22}]\text{-HMTADO})(\text{H}_2\text{O})_4]\text{Cl}_2 \cdot 8\text{H}_2\text{O}$ complex at room temperature were represented in Fig. 3. As shown these spectra exhibited one band at 584 nm due to the ${}^2\text{E}_g \rightarrow {}^2\text{T}_{2g}$ (O_h) transitions. The electronic absorption spectrum of $[\text{Cu}_2([\text{22}]\text{-HMTADO})(\text{H}_2\text{O})_4]^{2+}$ complex is typical of six-coordinate copper(II) complex. The symmetry of the octahedron, elongated or squashed along one axis, is D_{4h} , exactly that of the square plane. For tetragonal Cu^{2+} (d^9) complexes the octahedral doublet ${}^2\text{E}_g$ and ${}^2\text{T}_{2g}$ are seen to split as



The relative energies of the tetragonal components depend upon whether the octahedron is elongated or squashed, for ground state of elongated form is ${}^2\text{B}_{1g}$. Instead of the single ${}^2\text{E}_g \rightarrow {}^2\text{T}_{2g}$ transition which occurs for the regular octahedron, the tetragonally distorted molecule will exhibit two transitions ${}^2\text{B}_{1g} \rightarrow {}^2\text{B}_{2g}$ and ${}^2\text{B}_{1g} \rightarrow {}^2\text{E}_g$ at about the octahedral frequency [13]. A further band at much lower energy is expected from ${}^2\text{B}_{1g} \rightarrow {}^2\text{A}_{1g}$ transition [13].

The one $d-d$ band of title complexes observed at $17,123\text{ cm}^{-1}$ can be related to the spin-allowed transition, ${}^2\text{E}_g \rightarrow {}^2\text{T}_{2g}$. Copper complexes in tetragonal symmetry are expected to have three absorption bands in $d-d$ region, but title spectra apparently have one major component. Thus, we fitted the spectrum roughly with Gaussian functions first and then added a minor component to reproduce the

more suitable shape of the spectrum in the region of interest. Finally, we performed least-squares fitting procedures, and the dotted lines in Fig. 3 are Gaussian bands representing the approximate deconvolution of the spectrum yielded by the calculation. The two peak positions calculated at $15,506$ ($\epsilon = 61\text{ M}^{-1}\text{cm}^{-1}$) and $17,559\text{ cm}^{-1}$ ($\epsilon = 42\text{ M}^{-1}\text{cm}^{-1}$) can be assigned to the ${}^2\text{B}_{1g} \rightarrow {}^2\text{B}_{2g}$ and ${}^2\text{B}_{1g} \rightarrow {}^2\text{E}_g$, respectively. The ${}^2\text{B}_{1g} \rightarrow {}^2\text{A}_{1g}$ transition bands have expected at much lower energy. The $23,386\text{ cm}^{-1}$ ($\epsilon = 195\text{ M}^{-1}\text{cm}^{-1}$) bands are clearly associated with ligand to metal charge transfer transitions.

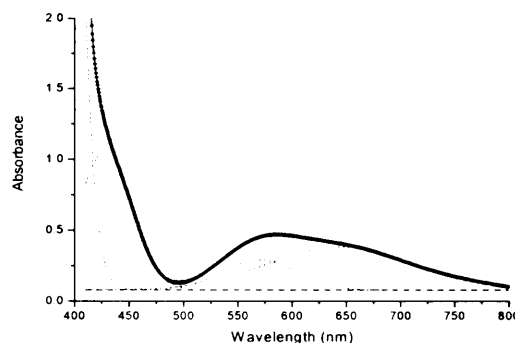


Fig. 3. Electronic absorption spectrum of $[\text{Cu}_2([\text{22}]\text{-HMTADO})(\text{OH}_2)_4]^{2+}$ in water.

3. Infrared spectra

IR spectra of the $[\text{Cu}_2([\text{22}]\text{-HMTADO})(\text{H}_2\text{O})_4]\text{Cl}_2 \cdot 8\text{H}_2\text{O}$ complexes were presented in Fig. 4. The strong and sharp absorption bands occurring at 1638 cm^{-1} are attributed to $\nu(\text{C}=\text{N})$ of the coordinated [22]-HMTADO ligand [14, 15], and the absence of any carbonyl bands associated with the diformylphenol starting materials or nonmacrocyclic

intermediates. The IR spectra displayed C-H stretching vibrations from 3000 to 2800 cm^{-1} . The present complexes exhibited three C-H deformation bands at 1440, 1390, and 1370 cm^{-1} regions and two out-of-plan vibration bands at 820 and 765 cm^{-1} regions. The bands occurring in the IR spectra of the complexes in the 3400-3550 cm^{-1} regions may probably be due to the $\nu(\text{OH})$ vibration of the coordinated and/or lattice water.

4. FAB mass spectra

The FAB mass spectra of the Cu(II) complexes were shown in Fig. 5. The FAB mass spectra of all the complexes contain peaks corresponding to the $[\text{Cu}_2(\text{[22]-HMTADO})]^+$ and $[\text{Cu}(\text{[22]-HMTADO})]^+$ ions at m/z 585 and 522, respectively. These major peaks are associated with peaks of mass one or two greater or less, which are attributed to protonated/deprotonated forms. This also accounts for the slight ambiguities in making assignments. The peak observed at m/z 620 is due to fragment $[\text{Cu}_2(\text{[22]-HMTADO})(\text{Cl})]^+$.

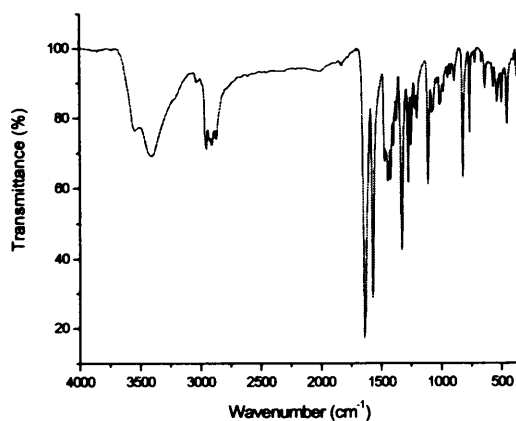


Fig. 4. FT-IR spectrum of $[\text{Cu}_2(\text{[22]-HMTADO})-(\text{OH}_2)]\text{Cl}_2 \cdot \text{H}_2\text{O}$.

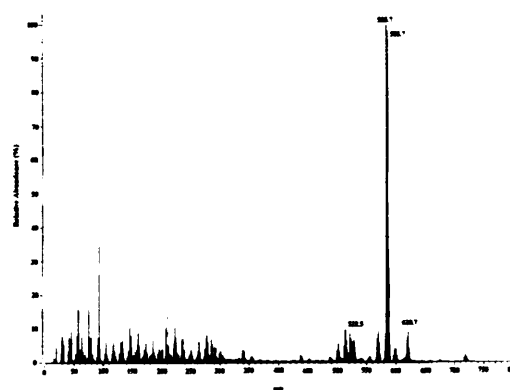


Fig. 5. FAB mass spectrum of the $[\text{Cu}_2(\text{[22]-HMTADO})(\text{OH}_2)]\text{Cl}_2 \cdot \text{H}_2\text{O}$.

Reference

- [1] B. Dietrich, P. Viout, and J. -M. Lehn, *Macrocyclic Chemistry*, VCH Verlagsgesellschaft, Weinheim, 1993.
- [2] J. -M. Lehn, *Supramolecular Chemistry*, VCH Verlagsgesellschaft, Weinheim, 1995.
- [3] E. C. Constable, *Metals and Ligand Reactivity*, VCH Verlagsgesellschaft, Weinheim, 1996.
- [4] J. R. Fredericks and A. D. Hamilton, in: A. D. Hamilton (Ed.), *Supramolecular Control of Structure and Reactivity*, Wiley, Chichester, 1996, Chapter 1.
- [5] J. W. Steed and J. L. Atwood, *Supramolecular Chemistry*, Wiley, Chichester, 2000.
- [6] (a) D. H. Bush, A. L. Vance and A. G. Kolochinskii, in: J. -M. Lehn (Ed.), *Comprehensive Supramolecular Chemistry*, vol. 9, Pergamon Press, 1996, Chapter 1; (b) N. V. Gerbeleu, V. B. Arion and J. Burges, *Template Synthesis of Macrocyclic Compounds*, Wiley-VCH, Weinheim, 1999.

- [7] S. M. Nelson, C. V. Knox, M. McCann, and M. G. B. Drew, *J. Chem. Soc., Dalton Trans.* **1981**, 1659.
- [8] W. Radecka-Paryzek, *Inorg. Chim. Acta* **1979**, 35, 349.
- [9] T. Shozo, *Bull. Chem. Soc. Jpn.* **1984**, 57, 2683.
- [10] J. C. Byun, Y. C. Park, and C. H. Han, *J. Kor. Chem. Soc.* **1999**, 43/3, 267.
- [11] Bruker, *SAINTPPLUS NT Version 5.0 Software Reference Manual Bruker AXS: Madison, Wisconsin, 1998.*
- [12] Bruker, *SHELXTL NT Version 5.16 Program for Solution and Refinement of Crystal Structures Bruker AXS: Madison, Wisconsin, 1998.*
- [13] D. Sutton, *Electronic Spectra of Transition Metal Complexes*, McGraw-Hill, London, **1968**.
- [14] L. A. Kahwa, J. Selbin, T. C. Y. Hsieh and R. A. Laine, *Inorg. Chim. Acta* **1986**, 118, 179.
- [15] D. Suresh Kumar and V. Alexander, *Inorg. Chim. Acta* **1995**, 238, 63.